Raman scattering by acoustic phonons in wurtzite ZnO prismatic nanoparticles

P.-M. Chassaing, F. Demangeot, and N. Combe
CNRS, CEMES (Centre d'Elaboration de Matériaux et d'Etudes Structurales), BP 94347, 29 Rue J. Marvig, 31055 Toulouse, France and Université de Toulouse, UPS, 31055 Toulouse, France

L. Saint-Macary, M. L. Kahn, and B. Chaudret
CNRS, LCC (Laboratoire de Chimie de Coordination), 205 Route de Narbonne, 31077 Toulouse, France
(Received 18 December 2008; revised manuscript received 11 February 2009; published 21 April 2009)

We report an observation by low-frequency Raman spectrometry of acoustic phonons in wurtzite prismatic zinc oxide nanoparticles of sizes varying from 2.3 to 6.6 nm. Several acoustic phonons confined in the nanoparticles are exhibited, shifting toward higher frequencies with a decrease in the nanoparticle size. We provide a comparison between experimental frequencies and those given by linear elasticity theory including both structural anisotropy and the specific shape of nanoparticles. We found that in addition to the usual breathing and fundamental extensional modes, spectra exhibit a peak attributed to the first harmonic of the extensional mode of nanoparticles.

DOI: 10.1103/PhysRevB.79.155314 PACS number(s): 78.30.Fs, 63.22.−m

I. INTRODUCTION

In the last twenty years, electronic quantum size effect (QSE) in semiconductor quantum dots (QDs) has been largely studied, and important optical device applications have been developed owing to their discrete atomiclike density of states. More recently, new semiconductors as III-nitride or II–VI compounds as zinc oxide (ZnO) have attracted a strong interest for the realization of UV optoelectronic devices operating at room temperature, since these materials have high band gap and large exciton binding energies. Moreover, effects of size reduction on exciton-LO (longitudinal optical) phonon coupling and the consequences on the emission process from InAs/GaAs QDs have been studied.[1,2] Detailed knowledge of acoustic phonons in QDs is also of strong importance, as it will help in the analysis of relaxation channels of electronic transitions at very low temperatures. For instance, acoustic modes interaction with excitons via deformation-potential mechanism can generate sidebands or phonon wings, resulting in an effective broadening of the zero-phonon line observable in single-dot spectroscopy measurements.[3,4] In particular, it is highly desirable to measure accurately confined acoustic phonon frequencies that need to be compared to the energy difference between confined states of the QDs. QDs are not so different from nanoparticles (NPs): QDs are commonly synthesized by physical methods, among all of them molecular-beam epitaxy, resulting in low aspect ratio nano-objects embedded in a solid. NPs are rather chemically synthesized, and can be self-standing objects with a tunable aspect ratio. QDs and NPs are close to each other because of common properties: for instance their nanometric scale, QSE, electron-phonon interaction, and vibrational properties. According to the synthesis method and properties of nano-objects we are focusing on, we will use in this article the term NPs.

ZnO NPs should be a very interesting system for single spectroscopy in the future since three-dimensional confinement can be reached with controlled NPs synthesis of typical size in the 4–6 nm range,[5,6] i.e., twice the exciton diameter of ZnO.[7] The study of carrier-phonon interaction in the strong-coupling regime could be lead in ZnO NPs, as long as one NP can be isolated. If numerous studies get interested in optical phonon modes in ZnO low-dimensional systems,[8–12] much less studies concern acoustic phonons. In this perspective, the present study is of high importance in order to know acoustic phonons energies in ZnO NPs.

Acoustic phonons in NPs can be probed by Raman[13,14] or pump-probe[15–18] spectroscopies. Coherent phonon measurements by pump-probe technique have been proved to be complementary to Raman scattering. Acoustic mode frequencies investigated by the two techniques are different, which illustrate the very different nature of light-matter interaction in Raman and time-resolved experiments:[17] the measured contributions of the different vibration modes and their relative intensities differ.

A previous work from Yadav *et al.*[13] reports Raman spectroscopy measurement of confined acoustic phonons on spherical ZnO NPs of sizes in the range 5.7–10.1 nm. The experimental frequencies are compared to those predicted by linear elasticity theory, assuming an isotropic stiffness tensor of ZnO. In the present work, we employ low-frequency Raman scattering to analyze size dependence of acoustic phonons confined in wurtzite prismatic ZnO NPs of size ranging from 2.3 to 6.6 nm. Experimental frequencies are compared to those computed with linear elasticity theory, taking into account the specific shape and elastic anisotropy of ZnO NPs.

II. NP SYNTHESIS AND CHARACTERIZATION

ZnO NPs were synthesized following an organometallic approach. This method takes advantage of the exothermic hydrolysis reaction of an organometallic precursor, $[Zn(Cy)_2]$, in presence of ligands as stabilizing agent, namely, long alkyl chain amine or a mixture of long alkyl chain amine and long alkyl chain carboxylic acid in an organic solvent. NPs synthesized are monocrystalline with a wurtzite structure, which is supported by x-ray diffraction measurements.[6]

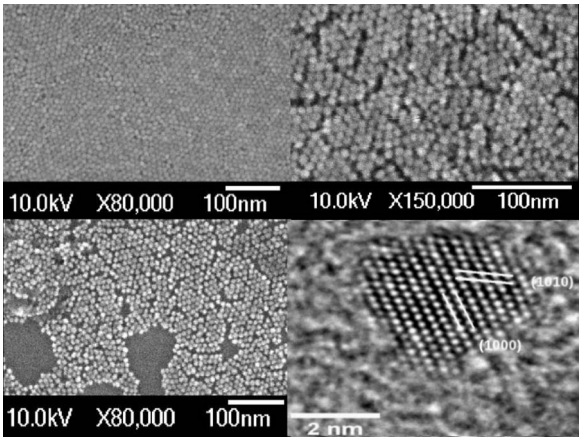

FIG. 1. SEM images of NPs synthesized following the route described in the text. On the bottom right, HRTEM image of a NP in the [0001] direction.

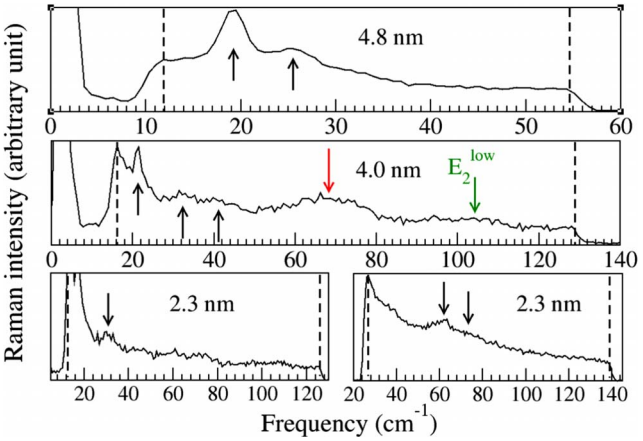

FIG. 2. (Color online) Low-frequency Raman spectra of three NPs from Table I. The spectral window is demarcated by dotted lines on each spectrum. Note that for the 2.3 nm NP, two acquisitions were made depending on the range of frequency, because of the very broad elastic scattering of this sample.

Another point of interest is the faceted hexagonal basis of NPs, as shown on the high-resolution transmission electron microscopy[19] (HRTEM) image of Fig. 1. This shape is a good approximation of the Wulff equilibrium shape for hcp crystals.[20] Moreover, scanning electron microscope[21] (SEM) images in Fig. 1 reveal the very good in-plane self-organization of NPs. Since we focus on the vibrational properties of NPs, no vibrational coherence effect resulting from their organization in supracrystals[22] has been investigated in this study. Details concerning prismatic shape control of NPs[23,24] and in plane self-organization[25] can be found elsewhere.

Nano-objects discussed here are constituted by a core of wurtzite ZnO, decorated by organic ligands bonded to the lateral surface of the NPs.[23,26] All NPs we studied have an aspect ratio of unity, which means they have a height H equal to their diameter D: $H=D=$Size. Detailed characteristics of NPs are given in Table I. The diameter of the NPs was determined from a histogram of sizes of ~200 NPs obtained via a transmission electron microscopy (TEM) image from top view of NPs (not shown). The histogram was fitted with a Gaussian curve which center and full width at half maximum gives, respectively, the mean diameter and standard deviation of Table I. In order to measure the height of NPs, a microtomy[27] of NPs was done so that one gets a transverse view of NPs with TEM observations. The determination of H from the TEM image of the transverse view is based on the same protocol as for D. As explained in Sec. IV, we explicitly take into account the specific shape and elastic anisotropy of wurtzite ZnO NPs in our calculations.

TABLE I. Characteristics of samples under study. Size is defined in the text. DDA=Dodecylamine, HDA=Hexadecylamine, OA=Octylamine.

Size ± std. dev. (nm)	1/size (nm^{-1})	Ligand
2.3 ± 0.5	0.435	DDA/lauric acid
2.9 ± 0.4	0.345	HDA/lauric acid
3.6 ± 0.6	0.278	HDA/octanoic acid
4.0 ± 0.9	0.250	OA/octanoic acid
4.8 ± 0.6	0.208	OA/lauric acid
5.6 ± 1.2	0.179	DDA
6.6 ± 1.2	0.152	OA

III. EXPERIMENTAL SETUP

Raman-scattering experiments were performed in air at room temperature using a T64000 Horiba-Jobin-Yvon spectrometer equipped with 2400 lines grating. In order to increase rejection of the spectrometer, classical backscattering geometry was replaced by a configuration where incoming laser light (413 nm, 3.00 eV) is focused on the sample under ~30° incidence, and scattered light is collected by a ×40 objective located on top of the sample surface.

IV. DISCUSSION

In Fig. 2 we show three typical spectra of NPs of size 2.3, 4.0, and 4.8 nm. The relevant signal obtained by the charge coupled device (CCD) detector is the area located between the two vertical dotted lines, which correspond to the boundaries of the spectral window of the spectrometer. This window was adjusted during experiments because of the variable scattering of incident light from one sample to the other (see Fig. 2). Following this scheme, we performed experiments on all NPs several times in a month in order to ensure the good reproducibility of our results.

Green arrow on Fig. 2 shows a weak and broad peak centered around ~100 cm^{-1} corresponding to the E_2 low-frequency phonon mode of ZnO.[28] Despite the focus on acoustic phonons of NPs, the observation of the E_2 mode evidences the presence of ZnO NPs. Note this mode is barely visible on Fig. 2 because of very large horizontal (vertical) scale dilatation (contraction). For each spectrum, black ar-

rows indicate two to three peaks shifting to higher frequencies when the size of NPs decreases. We attribute such peaks to vibration eigenmodes of NPs, and their shift with size reduction to confinement effect.[13] Note the frequency scale is not the same for all spectra. Origin of the peak marked by the red arrow at 69 cm^{-1} in 4 nm size NP, is still under discussion.

In a homogeneous elastic sphere, the most studied case, low-frequency vibration eigenmodes can be separated into two categories: spheroidal and torsional modes. In addition, these modes can be denoted by two integers n and l, which are, respectively, the harmonic and angular-momentum numbers. According to Duval,[29] only breathing ($l=0$) and quadrupolar ($l=2$) modes are Raman active. In the same paper, it is shown that breathing and quadrupolar modes obey different polarization selection rules, helping a lot in peak assignment on Raman spectra. However, these rules are true for spherical objects, and do not apply for prismatic wurtzite NPs. For NPs differing from spheres, breathing and quadrupolar modes remain the mostly observable modes thanks to their high interaction with electrons via deformation-potential mechanism. Indeed, breathing and quadrupolar modes have been widely reported in ZnO,[13] silver,[30,31] or gold[14] NPs of various shapes.

When considering prismatic NPs, the quadrupolar mode of a sphere leads to different modes:[32] among all of them, we focus on the extensional mode, which consists of a constriction of a section of the NP while the perpendicular direction is expanding, and vice versa. The breathing mode of a prismatic NP is similar to the one of a sphere. Another mode of interest is the first harmonic of the extensional mode. If breathing and fundamental extensional modes have been widely reported in literature,[13,15–17] we did not find any study identifying or evidencing the first harmonic of the extensional mode.

In this study, we aim to compare experimental frequencies to those obtained in the framework of linear elasticity theory. The latter were computed following the method of research of normal vibration modes of a free particle developed by Visscher *et al.*:[33] vibration displacements fields are developed on a polynomial basis so that resolution of the Navier equation reduces to linear algebra. We use in this study polynomials of order 11 to ensure the convergence of the method. This scheme was applied to wurtzite ZnO NPs shaped as a straight prism with a hexagonal basis using numerical values of density and elastic coefficients experimentally measured.[34] Note that neglecting the anisotropy of ZnO (not shown) would lead to an error of ~ 2 cm^{-1} on the value of the breathing and extensional frequencies for a 4 nm prismatic NP. To avoid misinterpretation in the mode attribution through Visscher scheme, breathing, fundamental extensional, and first harmonic were first calculated in an infinitely long isotropic cylinder so that their frequencies and displacement fields correspond to analytical solutions.[16] In a second time, we gradually decrease the aspect ratio H/D of the cylinder until it reaches 1 by following the three modes. Third, we include the anisotropy of the stiffness tensor, and finally we perform calculations on a prism with an aspect ratio of 1. In this case, the recognition of the modes is relatively easy because of the closeness of the cylindrical and prismatic shapes. Importantly, note that despite displacements associated to low-frequency eigenmodes of an infinite cylinder given in literature,[16,35–37] it is not the case to our knowledge for finite cylinders, so a direct recognition of the modes would be very fussy.

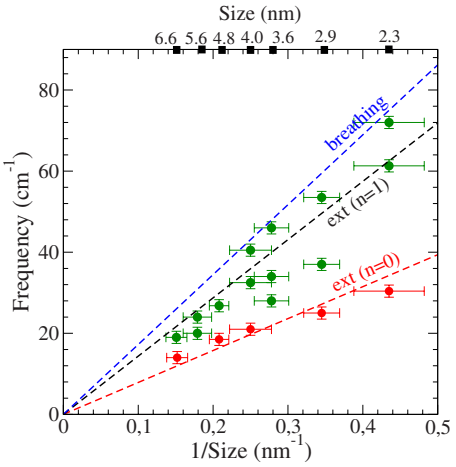

FIG. 3. (Color online) Experimental frequencies (full circles) and frequencies of breathing and extensional modes [fundamental ($n=0$) and first harmonics ($n=1$)] vs 1/size deduced from calculations in the framework of linear elasticity theory (dotted lines).

Figure 3 shows the comparison between experimental frequencies (full circles) and calculations following the method described above (dotted lines). As already mentioned, spectra exhibit two to three peaks shifting to higher frequencies when decreasing the size of NPs. In the following, we will thus refer to the low, intermediate, and high-frequency peaks for NPs showing three peaks (4.0, 3.6, and 2.9 and 2.3 nm), and to low and high-frequency peaks for other NPs (6.6, 5.6, and 4.8 nm). As seen on Fig. 3, the fundamental extensional mode ($n=0$) describes well the low-frequency peak (red circles), excepted for the 3.6 and 5.6 nm NPs. Note that we did not observe the fundamental extensional mode for these NPs. In addition, as one can see in Fig. 3, the line corresponding to the breathing mode (blue) is insufficient to reproduce other experimental data (green circles). More precisely, experimental frequencies agree well with breathing mode frequency for NPs with a size of 4.0, 3.6, and 2.3 nm, but fails to reproduce frequencies of other NPs. As suggested by Fig. 3, we attribute the high-frequency peak of NPs of size 6.6, 5.6, 4.8, and 2.9 nm and the intermediate frequency peak of NPs of size 4.0, 3.6, and 2.3 nm to the first harmonic of the extensional mode ($n=1$, black dotted line on Fig. 3). Attribution concerning the remaining peaks—i.e., the low peak for NPs of size 5.6 and 3.6 nm and the intermediate peak for the 2.9 nm NP, respectively—is still unclear. We want to point out our assignments are based on the closeness between the calculations based on elasticity theory and the experimental frequency, according to its error bars. As one can see in Fig. 3, the latter can be so important that two lines given by elasticity theory are contained in the error bars of the same experimental point. This is the case for the high-frequency peak of the 4.0 nm NP for example. As a consequence, our interpretation is not univocal and some of our assignments remain open to discussions.

A reason explaining the disagreement between experimental frequencies and those predicted by linear elasticity theory may come from the presence of ligands. Indeed, let us recall that NPs are coated by organic ligands as a result from their synthesis (see Table I): we recently pointed out the modification of optical phonons frequencies in ZnO NPs[10] due to ligands. A similar effect concerning acoustic phonons is not excluded, although the effect of surrounding medium on acoustic mode frequencies of NPs is still not clear.[38,39]

We recently theoretically investigated how surface effects modify structural and acoustic vibration properties of ZnO NPs similar to those reported in this study.[32] We provided a comparison between breathing and extensional mode frequencies determined by atomistic calculations and linear elasticity theory. Atomistic calculations implicitly take into account surface effects while linear elasticity does not. We evidenced that low-frequency vibration modes are inaccurately reproduced by theory of elasticity for NPs of size less than 2.5 nm because of surface effects. Results presented in this study are in agreement with this result since almost all NPs are greater than 2.5 nm and have eigenfrequencies quite well reproduced by linear elasticity theory. Only one NP is less than 2.5 nm, and as seen in Fig. 3, the corresponding experimental frequencies are not so far from those predicted by linear elasticity theory, according to the error bars. As a consequence, an observation of the alteration of vibration properties of NPs due to surface effects may require NPs smaller than 2.3 nm.

V. CONCLUSION

We report an experimental study on acoustic phonons in prismatic wurtzite ZnO NPs. Results of this study are interpreted in light of calculations in the framework of linear elasticity theory including both prismatic shape of NPs and anisotropy of elastic tensor of ZnO. We evidence three low-frequency eigenmodes of NPs, namely, the breathing, fundamental, and first harmonic of the extensional modes. Their experimental frequencies are rather well reproduced by linear elasticity theory, in spite of errors bars making some mode assignments not univocal. The first harmonic of the extensional mode is observed in the present study, although high-order (up to $n=4$) detection of breathing mode of a silver nanosphere has already been reported.[31] In addition, our results do not contradict our previous theoretical study concerning surface effects: the alteration of vibrational properties due to surface effects may be observable for NPs smaller than 2.3 nm.

[1] R. Heitz, I. Mukhametzhanov, O. Stier, A. Madhukar, and D. Bimberg, Phys. Rev. Lett. **83**, 4654 (1999).

[2] S. Hameau, Y. Guldner, O. Verzelen, R. Ferreira, G. Bastard, J. Zeman, A. Lemaître, and J.-M. Gérard, Phys. Rev. Lett. **83**, 4152 (1999).

[3] L. Besombes, K. Kheng, L. Marsal, and H. Mariette, Phys. Rev. B **63**, 155307 (2001).

[4] F. Rol, S. Founta, H. Mariette, B. Daudin, L. S. Dang, J. Bleuse, D. Peyrade, J. M. Gerard, and B. Gayral, Phys. Rev. B **75**, 125306 (2007).

[5] V. A. Fonoberov, K. A. Alim, A. A. Balandin, F. Xiu, and J. Liu, Phys. Rev. B **73**, 165317 (2006).

[6] M. L. Kahn, M. Monge, V. Collière, F. Senocq, A. Maisonnat, and B. Chaudret, Adv. Funct. Mater. **15**, 458 (2005).

[7] C. Jagadish and S. J. Pearton, *Zinc Oxide Bulk, Thin Films and Nanostructures* (Elsevier, New York, 2006), Vol. 1, p. 181.

[8] V. A. Fonoberov and A. A. Balandin, Phys. Rev. B **70**, 233205 (2004).

[9] V. A. Fonoberov and A. Balandin, J. Phys.: Condens. Matter **17**, 1085 (2005).

[10] P.-M. Chassaing, F. Demangeot, V. Paillard, A. Zwick, N. Combe, C. Pagès, M. L. Kahn, A. Maisonnat, and B. Chaudret, Phys. Rev. B **77**, 153306 (2008).

[11] H. M. Cheng, K. F. Lin, H. C. Hsu, and W. F. Hsieh, Appl. Phys. Lett. **88**, 261909 (2006).

[12] M. Rajalakshmi, A. K. Arora, B. S. Bendre, and S. Mahamuni, J. Appl. Phys. **87**, 2445 (2000).

[13] H. K. Yadav, V. Gupta, K. Sreenivas, S. P. Singh, B. Sundarakannan, and R. S. Katiyar, Phys. Rev. Lett. **97**, 085502 (2006).

[14] H. Portalès, L. Saviot, E. Duval, M. Fujii, S. Hayashi, N. Del Fatti, and F. Vallée, J. Chem. Phys. **115**, 3444 (2001).

[15] J. Margueritat, J. Gonzalo, C. N. Afonso, A. Mlayah, D. B. Murray, and L. Saviot, Nano Lett. **6**, 2037 (2006).

[16] M. Hu, X. Wang, G. V. Hartland, P. Mulvaney, J. P. Juste, and J. E. Sader, J. Am. Chem. Soc. **125**, 14925 (2003).

[17] J. Burgin, P. Langot, A. Arbouet, J. Margueritat, J. Gonzalo, C. N. Alfonso, F. Vallée, A. Mlayah, M. D. Rossell, and G. Van Tendeloo, Nano Lett. **8**, 1296 (2008).

[18] N. Del Fatti, C. Voisin, F. Chevy, F. Vallée, and C. Flytzanis, J. Chem. Phys. **110**, 11484 (1999).

[19] HRTEM was done with a JEOL JEM 2010 microscope (200 kV). NPs, consisting of a powder after synthesis, are dissolved into the organic solvent used during the synthesis. A drop of this solution is deposited on a very thin (20–30 nm) amorphous carbon layered copper grid. After solvent evaporation, a deposit containing NPs remains, which is dried under vacuum (1×10^{-5} torr) to remove all undesirable compounds.

[20] M. Touzani and M. Wortis, Phys. Rev. B **36**, 3598 (1987).

[21] SEM was done with a JEOL JSM 6700F microscope (10 kV). The powder containing NPs is deposited on a silicon substrate.

[22] A. Courty, A. Mermet, P. A. Albouy, E. Duval, and M. P. Pileni, Nature Mater. **4**, 395 (2005).

[23] M. Monge, M. L. Kahn, A. Maisonnat, and B. Chaudret, Angew. Chem. Int. Ed. **42**, 5321 (2003).

[24] A. Glaria, M. L. Kahn, T. Cardinal, F. Senocq, and B. Chaudret, New J. Chem. **32**, 662 (2008).

[25] M. L. Kahn, M. Monge, E. Snoeck, A. Maisonnat, and B. Chaudret, Small **1**, 221 (2005).

[26] M. L. Kahn, T. Cardinal, B. Bousquet, M. Monge, V. Jubera, and B. Chaudret, ChemPhysChem **7**, 2392 (2006).

[27] C. Pagès, PhD. Thesis, Université Paul Sabatier, Toulouse III, France, 2007.

[28] C. A. Arguello, D. L. Rousseau, and S. P. S. Porto, Phys. Rev. **181**, 1351 (1969).
[29] E. Duval, Phys. Rev. B **46**, 5795 (1992).
[30] G. Bachelier and A. Mlayah, Phys. Rev. B **69**, 205408 (2004).
[31] A. Nelet, A. Crut, A. Arbouet, N. Del Fatti, F. Vallée, H. Portalès, L. Saviot, and E. Duval, Appl. Surf. Sci. **226**, 209 (2004).
[32] N. Combe, P.-M. Chassaing, and F. Demangeot, Phys. Rev. B **79**, 045408 (2009).
[33] W. M. Visscher, A. Migliori, T. M. Bell, and R. A. Reinert, J. Acoust. Soc. Am. **90**, 2154 (1991).
[34] T. B. Bateman, J. Appl. Phys. **33**, 3309 (1962).
[35] A. E. Love, *Treatise on the Mathematical Theory of Elasticity*, 4th ed. (Dover, New York, 1944).
[36] E. P. Pokatilov, D. L. Nika, and A. A. Balandin, Superlattices Microstruct. **38**, 168 (2005).
[37] E. P. Pokatilov, D. L. Nika, and A. A. Balandin, Phys. Rev. B **72**, 113311 (2005).
[38] J. R. Huntzinger, A. Mlayah, V. Paillard, A. Wellner, N. Combe, and C. Bonafos, Phys. Rev. B **74**, 115308 (2006).
[39] L. Saviot, D. B. Murray, and M. C. Marco de Lucas, Phys. Rev. B **69**, 113402 (2004).